

## Research Communication

# Inhibitory Kinetics of $\beta$ -N-Acetyl-D-glucosaminidase from Prawn (*Litopenaeus vannamei*) by Zinc Ion

Xiao-Lan Xie<sup>1,2</sup>, Qian-Sheng Huang<sup>1</sup>, Min Gong<sup>1</sup>, Juan Du<sup>1</sup>, Yi Yang<sup>3</sup> and Qing-Xi Chen<sup>1</sup>

<sup>1</sup>Key Laboratory of Ministry of Education for Cell Biology and Tumor Cell Engineering, School of Life Sciences, Xiamen University, Xiamen, China

<sup>2</sup>School of Chemistry and Life Sciences, Quanzhou Normal University, Quanzhou, China

<sup>3</sup>School of Pharmacy, East China University of Science and Technology, Shanghai, China

### Summary

Prawn (*Litopenaeus vannamei*)  $\beta$ -N-acetyl-D-glucosaminidase (NAGase, EC 3.2.1.52) is involved in the digestion and molting processes. Zinc is one of the most important metals often found in the pollutant. In this article, the effects of  $\text{Zn}^{2+}$  on prawn NAGase activity for the hydrolysis of pNP-NAG have been investigated. The results showed that  $\text{Zn}^{2+}$  could reversibly and noncompetitively inhibit the enzyme activity at appropriate concentrations and its  $\text{IC}_{50}$  value was estimated to be  $6.00 \pm 0.25$  mM. The inhibition model was set up, and the inhibition kinetics of the enzyme by  $\text{Zn}^{2+}$  has been studied using the kinetic method of the substrate reaction. The inhibition constant was determined to be 11.96 mM and the microscopic rate constants were also determined for inactivation and reactivation. The rate constant of the inactivation ( $k_{+0}$ ) is much larger than that of the reactivation ( $k_{-0}$ ). Therefore, when the  $\text{Zn}^{2+}$  concentration is sufficiently large, the enzyme is completely inactivated. On increasing the concentration of  $\text{Zn}^{2+}$ , the fluorescence emission peak and the UV absorbance peak are not position shifted, but the intensity decreased, indicating that the conformation of  $\text{Zn}^{2+}$ -bound inactive NAGase is stable and different from that of native NAGase. We presumed that  $\text{Zn}^{2+}$  made changes in the activity and conformation of prawn NAGase by binding with the histidine or cysteine residues of the enzyme. © 2008 IUBMB

IUBMB *Life*, 61(2): 163–170, 2009

**Keywords**  $\beta$ -N-acetyl-D-glucosaminidase; *Litopenaeus vannamei*; kinetics; zinc ions; inhibition.

**Abbreviations**  $\text{IC}_{50}$ , the inhibitor concentration leading to 50% of enzyme activity lost; NaAc-HAc buffer, sodium acetate and acetic acid buffer;

NAG, N-acetylglucosamine; NAGase,  $\beta$ -N-acetyl-D-glucosaminidase; pNP, p-nitrophenol; pNP-NAG, p-nitrophenyl-N-acetyl- $\beta$ -D-glucosaminide;  $\text{Zn}^{2+}$ , zinc ion;  $\text{ZnSO}_4$ , zinc sulfate.

### INTRODUCTION

Chitin, a mucopolysaccharide polymer consisting of  $\beta$ -1,4-linked N-acetylglucosamine (NAG) residues, is one of the most abundant carbohydrates present in the marine environment. Biological decomposition of chitin has been widely studied during the last 20 years as a promising way to use chitin. The degradation of chitin into NAG is achieved by the synergistic action of endochitinase, exochitinase, and  $\beta$ -N-acetyl-D-glucosaminidase (NAGase, EC 3.2.1.52). Moreover, chitinase and NAGase play important roles in defense systems against parasites, molting, and digestion of chitinous foods (1–4). Chitinase and NAGase from crustaceans are involved not only in the molting process but also in hatching (5). Much dramatic progress in NAGase studies, including cloning and expressing of a large number of NAGase genes, has been made in recent years (6, 7). The purification, concentrations in different growth stage, and distribution in different organs of the NAGases from Antarctic krill (8, 9), lobster (*Homarus americanus*) (10), fiddler crab (*Uca pugilator*) (11), and Northern shrimp (*Pandalus borealis*) (12) have been reported. NAGases from Antarctic krill exist as two isoenzymes which are involved in digestion and molting processes, respectively. Their simultaneous occurrence may indicate a physiological adaptation utilizing a mechanism of altering isoenzyme concentrations (8, 9). The prawn *Litopenaeus vannamei* is one of the most popular farmed prawns in the world. Currently, systematical studies of NAGase from *L. vannamei* are taking place in our laboratory (13–16).

Prawn aquaculture has increased rapidly from an insignificant base in the early 1980s, to a multibillion dollar industry in

Received 18 June 2008; accepted 12 August 2008

Address correspondence to: Qing Xi Chen, Key Laboratory of Ministry of Education for Cell Biology and Tumor Cell Engineering, School of Life Sciences, Xiamen University, Xiamen 361005, China. Tel: +86-592-2185487. Fax: +86-592-2185487. E-mail: chenqx@xmu.edu.cn

the recent years. However, the commercial culture of prawn (*L. vannamei*) has been hampered because of stressful environments such as change in salinity, high concentrations of ammonia, high concentrations of organic solvents, and heavy metal ions (17). Heavy metal contamination has been identified as a concern in coastal environment because of discharges from industrial wastes and agricultural and urban sewage. Zinc is one of the most important metals often found in the pollutants. Although zinc plays an important role in biological systems, it can also produce toxic effects on the enzyme activity and its conformation and on the growth and survival of the animal when zinc intake is excessively elevated. So it is very important to research the influence of zinc ions on the *L. vannamei* NAGase activity. In our investigation, we found that *L. vannamei* NAGase activity could be affected by  $Zn^{2+}$ , and the inhibition of the enzyme by  $Zn^{2+}$  was shown to be reversible. Therefore, the aim of this article is to concentrate on the kinetics of inhibition of the enzyme by  $Zn^{2+}$  using the substrate reaction kinetics method described by Tsou (18) and Xie et al. (19), and to similarly measure the rate constants of reversible inactivation and reactivation.

## MATERIALS AND METHODS

### Materials

NAGase (EC 3.2.1.52) was prepared from prawn (*L. vannamei*) as described previously (14). The specific activity of the purified enzyme was 1,560 U/mg. *p*-Nitrophenyl-*N*-acetyl- $\beta$ -D-glucosaminide (*p*NP-NAG) was purchased from the Biochemistry Lab of Shanghai Medicine Industry Academy (China). Zinc sulfate ( $ZnSO_4$ ) and all other reagents were local products of analytical grade. The water used was redistilled and ion-free.

### Assay

Enzyme concentration was measured by the method of Lowry et al. (20). Enzyme activity was determined at 37 °C by measuring the increasing absorbance at 405 nm accompanying the hydrolysis of the substrate (*p*NP-NAG) (14). A portion of 10  $\mu$ L of enzyme solutions was added to the reaction media (2.0 mL) containing 0.5 mM *p*NP-NAG in 0.1 M NaAc-HAc buffer (pH 5.8). Absorption was carried out using a Beckman UV-650 spectrophotometer. The molar absorption coefficient of the product (pNP) was determined to be  $1.77 \times 10^3$  ( $M^{-1} cm^{-1}$ ) at pH 5.8.

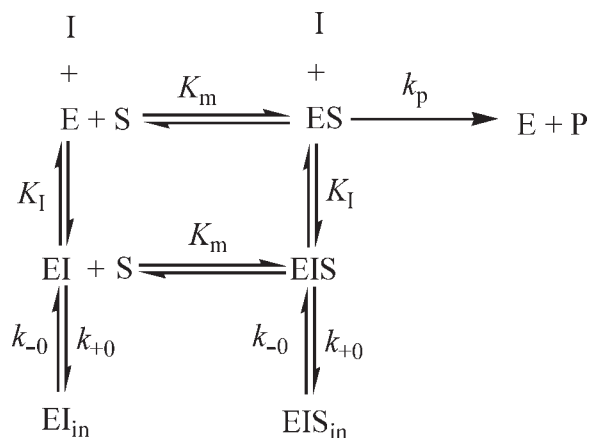
Fluorescence spectra were measured with a Hitachi 4010 spectrophotometer. Twenty-five micrograms of prawn NAGase was dissolved in 1.0 mL of 0.1 M NaAc-HAc buffer (pH 5.8) containing different  $Zn^{2+}$  concentrations at 37 °C. The enzyme was preincubated for 2 min before taking the fluorescence spectra measurements at an excitation wavelength of 280 nm.

A Beckman DU 650 spectrophotometer was used to measure the UV absorbance spectra of the enzyme which was treated with different concentrations of  $Zn^{2+}$  in 0.1 M NaAc-HAc buffer (pH 5.8) for 10 min.

### Inactivation Rate Constants of Prawn NAGase by $Zn^{2+}$

The progress-of-substrate reaction method previously described by Tsou (18) and Xie et al. (19) was applied to the study of the inhibition kinetics of prawn NAGase by  $Zn^{2+}$ . In this method, 10  $\mu$ L of enzyme was added to 2.0 mL assay system containing different concentrations of substrate in 0.1 M NaAc-HAc buffer (pH 5.8) with different concentrations of  $Zn^{2+}$ . The enzyme activity was monitored for absorbance at 405 nm, each minute for 60 min. The relation between the amount of the product (pNP) and the reaction time was figured into the substrate reaction progress curve in the time course of the hydrolysis of the substrate catalyzed by prawn NAGase in the presence of  $Zn^{2+}$  at different concentrations at 37 °C. The amount of the product (pNP) was denoted using the absorbance at 405 nm. The substrate reaction progress curve was analyzed to obtain the reaction rate constants as detailed below.

For slow, reversible, and noncompetitive inhibition with fractional residue activity, the kinetic model of the enzyme reacting with the substrate and the inhibitor can be written as (16)



E, S, I, and P denote enzyme, substrate, inhibitor ( $Zn^{2+}$ ), and product, respectively. EI, ES, and EIS are the respective complexes.  $EI_{in}$  and  $EIS_{in}$  are inactive enzyme forms.  $K_I$  is the equilibrium binding constant for the inhibitor ( $Zn^{2+}$ ), and  $k_{+0}$  and  $k_{-0}$  are the rate constants for inactivation and reactivation of the enzyme, respectively.

As is usually the case  $[S] \gg [E_0]$ ,  $[I] \gg [E_0]$ , and the inhibition reactions are relatively slow compared with the setup of the steady-state of the enzymatic reaction,

$$\begin{aligned}
 [E] &= \frac{K_I K_m}{(K_I + [I])(K_m + [S])} [E_T] \\
 [ES] &= \frac{K_I [S]}{(K_I + [I])(K_m + [S])} [E_T] \\
 [EI] &= \frac{K_m [I]}{(K_I + [I])(K_m + [S])} [E_T] \\
 [EIS] &= \frac{[I][S]}{(K_I + [I])(K_m + [S])} [E_T]
 \end{aligned} \tag{1}$$

where  $[E_T] = [E] + [ES] + [EI] + [EIS]$  and  $[E_T^*] = [EI_{in}] + [EIS_{in}]$  are the total concentration of the active and inactive enzymes, respectively.  $[E_0] = [E_T] + [E_T^*]$ , and  $K_m$  is the Michaelis constant. The decrease rate of  $E_T$  can be given in the following form:

$$\begin{aligned} -\frac{d[E_T]}{dt} &= \frac{d[E_T^*]}{dt} \\ &= k_{+0}([EI] + [EIS]) - k_{-0}([EI_{in}] + [EIS_{in}]) \\ &= k_{+0}([EI] + [EIS]) - k_{-0}[E_T^*] \\ &= A[E_T] - B[E_0] \end{aligned} \quad (2)$$

where

$$A = \frac{k_{+0}[I]}{K_I + [I]} + k_{-0} \quad \text{and} \quad B = k_{-0} \quad (3)$$

$A$  and  $B$  are the apparent rate constants for inhibition and reactivation, respectively. The product formation can be written as

$$[P]_t = \frac{k_{-0}v}{A} \cdot t + \frac{(A - k_{-0})v}{A^2} (1 - e^{-A \cdot t}) \quad (4)$$

where  $[P]_t$  is the product concentration formed at reaction time  $t$ , and  $v$  is the initial reaction rate in the absence of  $Zn^{2+}$ . When  $t$  is sufficiently large, the curves become straight lines and the product concentration is written as  $[P]_{calc}$ :

$$[P]_{calc} = \frac{k_{-0}v}{A} \cdot t + \frac{(A - k_{-0})v}{A^2} \quad (5)$$

A plot of  $[P]_{calc}$  versus  $t$  gives a straight line with

$$\text{Slope} = \frac{k_{-0}v}{A} \quad (6)$$

Combining Eqs. (4) and (5) gives

$$[P]_{calc} - [P]_t = \frac{(A - k_{-0})v}{A^2} \cdot e^{-A \cdot t} \quad (7)$$

$$\ln([P]_{calc} - [P]_t) = \ln \frac{(A - k_{-0})v}{A^2} - A \cdot t \quad (8)$$

Plots of  $\ln([P]_{calc} - [P]_t)$  versus  $t$  give a series of straight lines with slopes of  $-A$  at different  $Zn^{2+}$  concentrations. A plot of  $[P]_{calc}$  versus  $t$  gives a straight line with a slope of  $vk_{-0}/A$  which can be used to determine  $k_{-0}$ .

The apparent forward rate constant,  $A$ , is independent of the substrate concentration, but it depends on the  $Zn^{2+}$  concentration  $[I]$ . From Eq. (3), the following equation is obtained.

$$\frac{1}{A - k_{-0}} = \frac{K_I}{k_{+0}} \cdot \frac{1}{[I]} + \frac{1}{k_{+0}} \quad (9)$$

A plot of  $1/(A - k_{-0})$  versus  $1/[I]$  gives a straight line with a slope of  $K_I/k_{+0}$  and an intercept of  $1/k_{+0}$  on the ordinate and  $-1/K_I$  on the abscissa, which can be used to determine the microscopic rate constant,  $k_{+0}$ , and the equilibrium binding constant for the  $Zn^{2+}$ ,  $K_I$ .

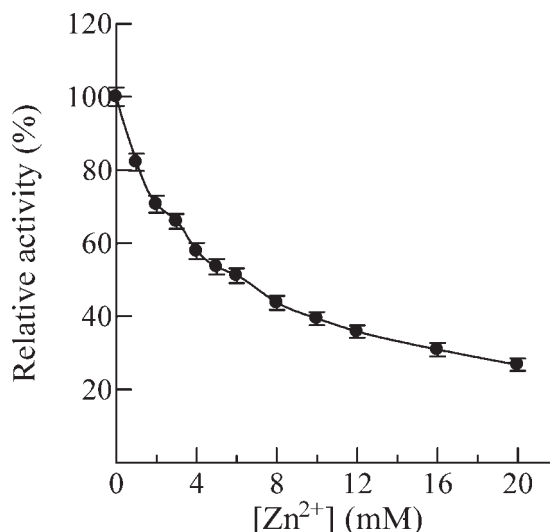


**Figure 1.** Effect of  $Zn^{2+}$  on the activity of NAGase for the hydrolysis of pNP-NAG. Conditions used were 2 mL system containing 0.1 M NaAc-HAc buffer (pH 5.8) and 0.5 mM substrate at 37 °C. The enzyme's final concentration was 0.0075  $\mu$ M.

## RESULTS

### Determination of the Kinetic Parameters of Prawn NAGase

The kinetic behavior of prawn NAGase in catalyzing the hydrolysis of pNP-NAG has been studied. Under the condition employed in this investigation, the hydrolysis of pNP-NAG by prawn NAGase follows Michaelis–Menten kinetics. The kinetic parameters of prawn NAGase were obtained from a Lineweaver–Burk plot showing that  $K_m$  was equal to  $0.255 \pm 0.015$  mM and  $V_m$  was equal to  $6.855 \pm 0.205$   $\mu$ M/min.

### Effects of $Zn^{2+}$ on the Activity of Prawn NAGase

The effect of  $Zn^{2+}$  on the hydrolysis of pNP-NAG by prawn NAGase was first studied. Figure 1 shows the relationship of residual enzyme activity and  $Zn^{2+}$  concentrations. The effect of  $Zn^{2+}$  on enzyme activity was concentration dependent. As the concentration of  $Zn^{2+}$  increased, the residual enzyme activity decreased rapidly. The value of  $IC_{50}$ ,  $Zn^{2+}$  concentration leading to 50% activity lost, was estimated to be  $6.00 \pm 0.25$  mM. The inhibition mechanism of  $Zn^{2+}$  on the enzyme activity was studied in the lower  $Zn^{2+}$  concentrations. Figure 2 shows the relationship of enzyme activity and its concentration in the presence of different  $Zn^{2+}$  concentrations. The plots of the remaining enzyme activity versus the concentrations of enzyme in the presence of different  $Zn^{2+}$  concentrations gave a family of straight lines, which all passed through the origin. Increasing the  $Zn^{2+}$  concentration resulted in the descending of the slope of the line, indicating that the inhibition of  $Zn^{2+}$  on the enzyme was a reversible reaction course. The abscissa intercept kept the same (zero), suggesting that the presence of  $Zn^{2+}$  did not bring

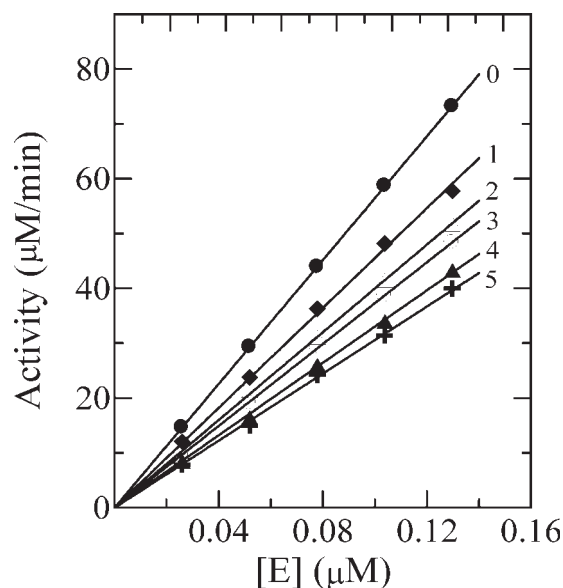


**Figure 2.** Effects of NAGase concentration on its activity for the hydrolysis of pNP-NAG at different concentrations of  $\text{Zn}^{2+}$ . The concentrations of  $\text{Zn}^{2+}$  for curves 0–5 were 0, 1, 2, 3, 4, and 5 mM, respectively. Assay conditions used were the same as in Fig. 1.

down the amount of the efficient enzyme, but it just resulted in the inhibition and the descending of the activity of the enzyme.  $\text{Zn}^{2+}$  is a reversible inhibitor of prawn NAGase.

The inhibition model of enzyme by  $\text{Zn}^{2+}$  was determined by the standard Lineweaver–Burk plot of  $1/v$  versus  $1/[S]$  for different concentrations of the inhibitor. The results showed that the value of  $K_m$  was unchanged and that of  $V_m$  was changed in the presence of different  $\text{Zn}^{2+}$  concentrations, suggesting that  $\text{Zn}^{2+}$  was a noncompetitive inhibitor. The equilibrium constant for  $\text{Zn}^{2+}$  binding enzyme  $K_I$  and the values of  $k_{\text{cat}}$  in the presence of different  $\text{Zn}^{2+}$  concentrations were determined and summarized in Table 1.

### Kinetics of the Substrate Reaction In the Presence of Different $\text{Zn}^{2+}$ Concentrations

The progress-of-substrate reaction method previously described by Tsou (18) and Xie et al. (19) was used to study the inhibition kinetics of  $\text{Zn}^{2+}$  on prawn NAGase. The time course of the hydrolysis of the substrate in the presence of different  $\text{Zn}^{2+}$  concentrations was shown in Fig. 3a. At each  $\text{Zn}^{2+}$  concentration, the rate decreased with increasing time until a straight line was approached. The results showed that at a certain  $\text{Zn}^{2+}$  concentration, the inhibition was a reversible reaction with fractional residual activity and the substrate gave very little protection. A plot of  $[P]_{\text{calc}}$  against  $t$  gave a series of straight lines with slopes of  $(vk_{-0}/A)$  at different  $\text{Zn}^{2+}$  concentrations according to Eq. (5), and plot of  $\ln([P]_{\text{calc}} - [P]_t)$  against  $t$  gave a series of straight lines with slopes of  $-A$  at different  $\text{Zn}^{2+}$  concentrations as shown in Fig. 3b. The dependence of  $A$  on the  $\text{Zn}^{2+}$  concentration was fit using a second-order least squares fit (Fig. 3c). The intercept of the curve on the ordinate gave the value of  $k_{-0}$ , the microscopic rate constant of the reactivation of the enzyme, which was  $1.26 \times 10^{-2} \text{ min}^{-1}$  and listed in Table 1. The value of  $k_{-0}$  was almost the same for different  $\text{Zn}^{2+}$  concentrations. From Eq. (9), a plot of  $1/(A - k_{-0})$  against  $1/[I]$  gave a straight line (Fig. 4). The intercepts of straight line on the ordinate and on the abscissa gave the values of  $1/k_{+0}$  and  $-1/K_I$ , respectively. The equilibrium constant for  $\text{Zn}^{2+}$  binding enzyme,  $K_I$ , was determined to be 11.96 mM. And the microscopic rate constant for inactivation,  $k_{+0}$ , was determined to be  $32.96 \times 10^{-2} \text{ min}^{-1}$ . These results are shown in Table 1.

### Kinetics of the Reaction at Different Substrate Concentrations In the Presence of $\text{Zn}^{2+}$

Figure 5a showed the kinetic courses of the reaction at different pNP-NAG concentrations in the presence of 1 mM  $\text{Zn}^{2+}$ . Similarly, plots of  $\ln([P]_{\text{calc}} - [P]_t)$  against  $t$  gave a family of straight lines with slopes of  $-A$  at different substrate concentrations as shown in Fig. 5b. The apparent forward rate constants,

**Table 1**  
Inhibition parameters for NAGase by  $\text{Zn}^{2+}$

| $[\text{Zn}^{2+}]$<br>(mM) | $1/[\text{Zn}^{2+}]$ | $k_{\text{cat}}$<br>( $\text{min}^{-1}$ ) | $A$<br>( $\text{min}^{-1}$ ) | $vk_{-0}/A$<br>( $\text{min}^{-1}$ ) | $k_{-0}$<br>( $\text{min}^{-1}$ ) | $A - k_{-0}$ | $1/(A - k_{-0})$ | $k_{+0}$ ( $\text{min}^{-1}$ ) | $K_I$ (mM)                               |
|----------------------------|----------------------|---|------------------------------|--------------------------------------|-----------------------------------|--------------|------------------|--------------------------------|--|
| 0                          | 0                    | 913.98                                    |                              |                                      |                                   |              |                  |                                |  |
| 1                          | 1                    | 811.32                                    | 0.038                        | 0.0017                               | $1.26 \times 10^{-2}$             | 0.0254       | 39.29            | $32.96 \times 10^{-2}$         | 11.92 <sup>a</sup><br>11.96 <sup>b</sup> |
| 2                          | 0.5                  | 775.17                                    | 0.059                        | 0.00154                              |                                   | 0.0473       | 21.16            |                                |  |
| 3                          | 0.333                | 717.79                                    | 0.078                        | 0.00148                              |                                   | 0.0661       | 15.12            |                                |  |
| 4                          | 0.25                 | 661.32                                    | 0.095                        | 0.00135                              |                                   | 0.0827       | 12.09            |                                |  |
| 5                          | 0.2                  | 587.28                                    | 0.109                        | 0.00126                              |                                   | 0.0972       | 10.29            |                                |  |

<sup>a</sup>Obtained from Lineweaver–Burk plots.

<sup>b</sup>Obtained from the plot of  $1/(A - k_{-0})$  versus  $1/[I]$ .

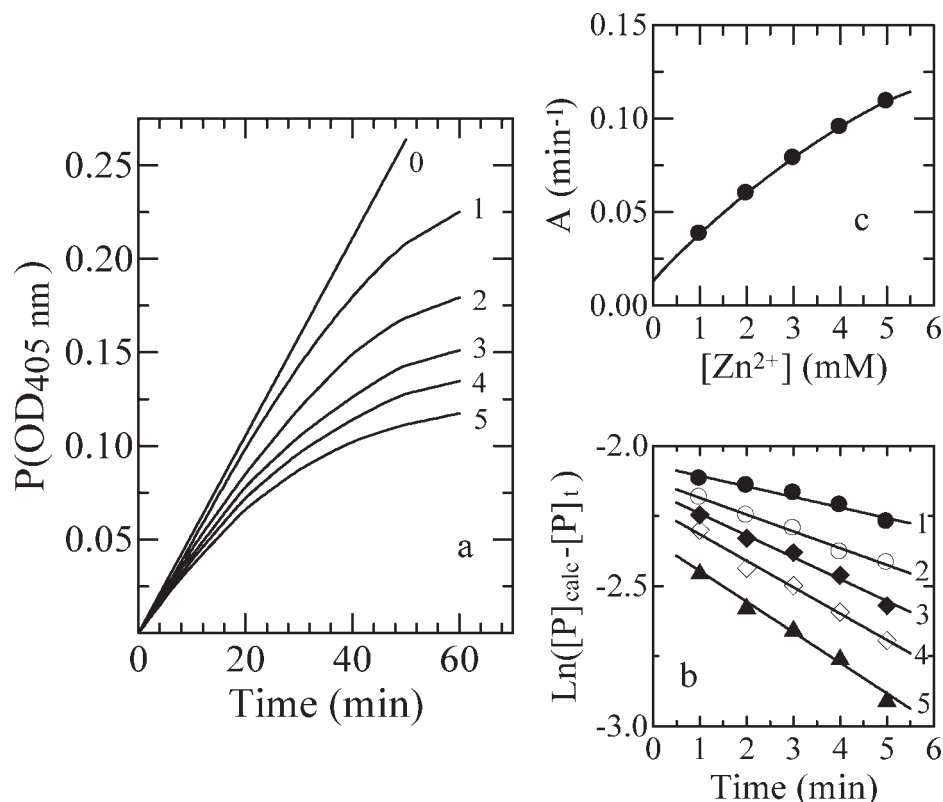


**Figure 3.** Inhibition kinetics for prawn (*Litopenaeus vannamei*) NAGase at various concentrations of  $\text{Zn}^{2+}$ . (a) Course of the substrate reaction in the presence of different  $\text{Zn}^{2+}$  concentrations. The final enzyme concentration was  $0.0075 \mu\text{M}$ . The reaction mixture (2.0 mL) contained 0.25 mM pNP-NAG and varying concentrations of  $\text{Zn}^{2+}$  in 0.1 M NaAc-HAc buffer at pH 5.8. The  $\text{Zn}^{2+}$  concentrations for curves 0–5 were 0, 1, 2, 3, 4, and 5 mM, respectively. (b) Semilogarithmic plot of  $\ln([P]_{\text{calc}} - [P]_t)$  against time; the data were taken from curves 1–5 of (a). (c) The apparent forward inhibition rate constants for various  $\text{Zn}^{2+}$  concentrations; the data were taken from curves 1–5 of (b).

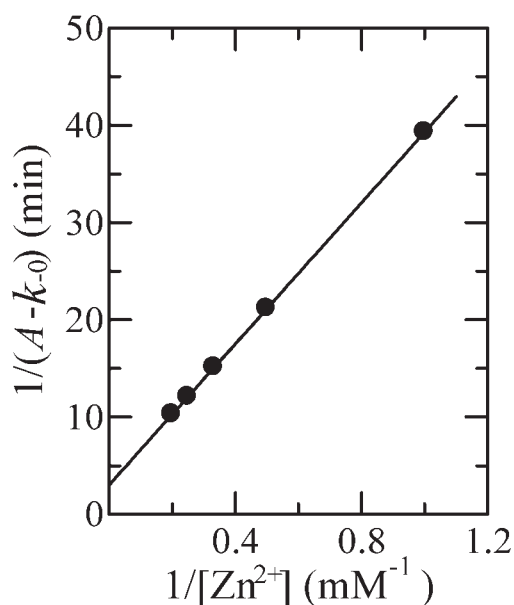


**Figure 4.** Plot of  $1/(A - k_{-0})$  versus  $1/[\text{Zn}^{2+}]$ .

$A$ , could be obtained through suitable plots. A plot of the slopes of the straight lines in Fig. 5b against the substrate concentration  $[S]$  gave a horizontal straight line (Fig. 5c), indicating that the substrate concentration did not affect the microscopic rate constants:  $k_{+0}$  and  $k_{-0}$ . The result proved that  $\text{Zn}^{2+}$  was a non-competitive inhibitor of the enzyme.

#### Fluorescence Emission Spectra of Prawn NAGase Inactivated by $\text{Zn}^{2+}$

The fluorescence emission spectra of prawn NAGase in different  $\text{Zn}^{2+}$  concentrations were determined and the results are shown in Fig. 6. The emission peak of the native enzyme at 338 nm may contain contributions from both Trp and Tyr residues. The fluorescence emission intensity gradually decreased with increasing  $\text{Zn}^{2+}$  concentrations without significant position-shift of emission peak. The results showed that the microenvironments of both Trp and Tyr residues of the enzyme had obviously changed after inactivation by  $\text{Zn}^{2+}$ .



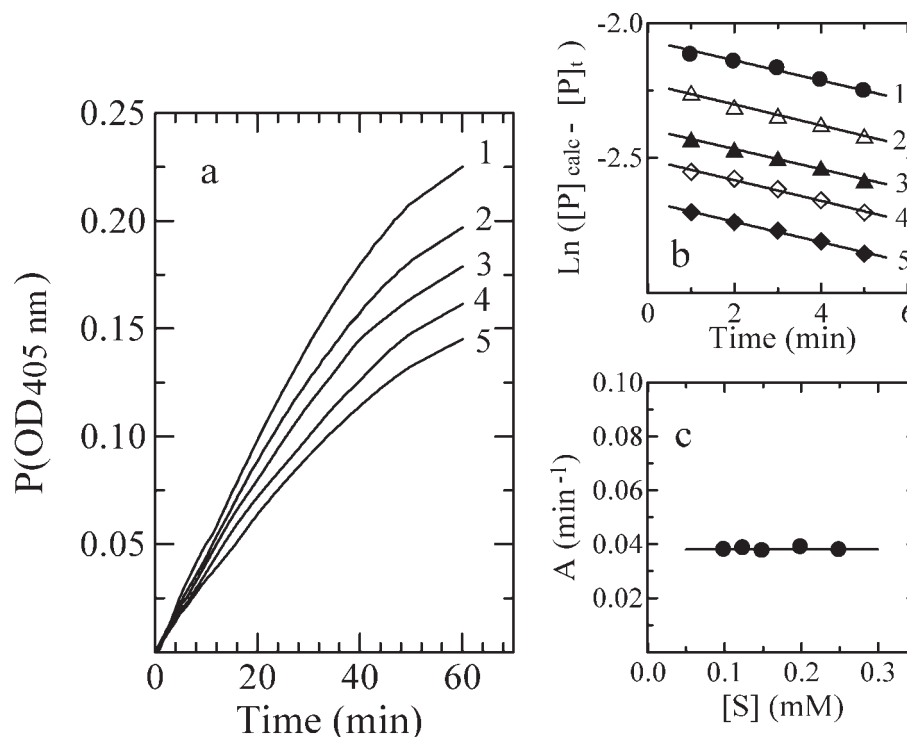


**Figure 5.** Course of the substrate reaction at different substrate concentrations in the presence of  $\text{Zn}^{2+}$ . The final  $\text{Zn}^{2+}$  concentration was 1 mM and the final enzyme concentration was  $0.0075 \mu\text{M}$ . Experimental conditions were the same as in Fig. 3 except for the pNP-NAG concentration. (a) Curves 1–5 are progress curves for substrate concentrations of 0.25, 0.20, 0.15, 0.125, 0.10 mM, respectively. (b) Semilogarithmic plot of  $\ln([P]_{\text{calc}} - [P]_t)$  against time, with the data taken from curves 1–5 of (a). (c) Plot of the apparent forward inhibition rate constants  $A$  versus substrate concentrations.

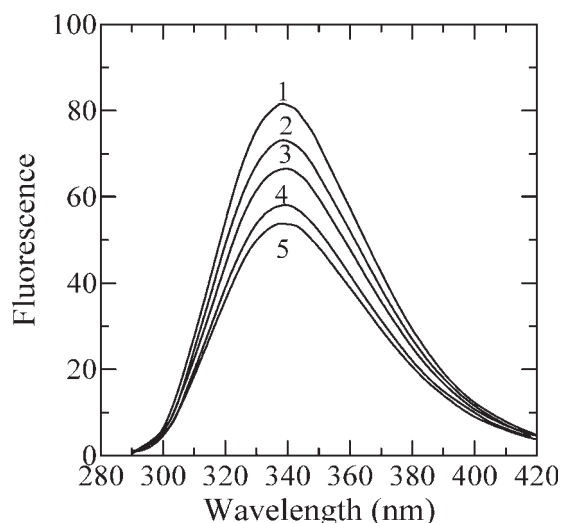


**Figure 6.** Fluorescence emission spectra of *Litopenaeus vannamei* NAGase in  $\text{Zn}^{2+}$  solution. The final concentrations of  $\text{Zn}^{2+}$  were 0, 2.5, 5.0, 7.5, and 10.0 mM for curves 1–5, respectively. The final enzyme concentration was  $25 \mu\text{g/mL}$ .

#### UV Absorbance Spectra of Prawn NAGase Inactivated by $\text{Zn}^{2+}$

The conformational changes of the enzyme after inactivation by  $\text{Zn}^{2+}$  were studied using UV absorbance spectra. The UV absorbance spectra of the enzyme after incubation in different  $\text{Zn}^{2+}$  concentration solutions for 10 min were determined and the results are shown in Fig. 7. The native enzyme had a characteristic absorbance peak at 276 nm (curve 1 in Fig. 7). For the native enzyme, the UV absorbance peak at 276 nm may also be contributed by the residues Trp and Tyr. The absorbance intensity at 276 nm slowly decreased with increasing  $\text{Zn}^{2+}$  concentrations, indicating that the microenvironments of both Trp and Tyr residues of the enzyme had changed after inactivation by  $\text{Zn}^{2+}$ . The results obtained from UV absorbance spectra were accordant with those obtained from fluorescence emission spectra.

#### DISCUSSION

$\text{Zn}^{2+}$  contributes to a wide variety of important biological processes including gene expression, replication, and hormonal

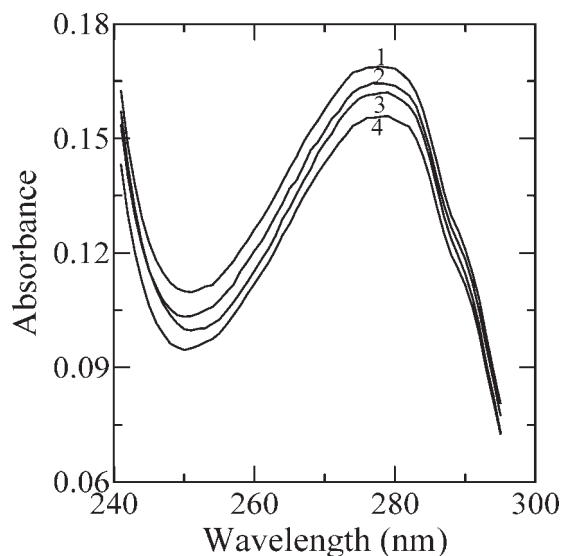


**Figure 7.** Ultraviolet absorption spectra of *Litopenaeus vannamei* NAGase in  $\text{Zn}^{2+}$  solution. The final concentrations of  $\text{Zn}^{2+}$  were 0, 5.0, 10.0, and 15.0 mM for curves 1–4, respectively. The final enzyme concentration was 25  $\mu\text{g/mL}$ .

storage and release. It is also critical for the structural integrity of cells, influencing membrane stability and cytoskeletal organization. However, excess  $\text{Zn}^{2+}$  is also associated with a number of abnormalities and neurodegenerative disorders of organisms (21). We had tested the effects of  $\text{Zn}^{2+}$  on prawn NAGase activity *in vivo*. The results showed that the NAGase activity had no marked change when the prawn was bred in sea water containing 0.015 mM  $\text{Zn}^{2+}$  for 1 day, whereas the NAGase activity markedly decreased when the prawn was bred in sea water containing 0.015 mM  $\text{Zn}^{2+}$  for 3 days. This finding inspired us to lucubrate about the inhibitory mechanism of  $\text{Zn}^{2+}$  on prawn NAGase. So we purified the prawn NAGase (14) and studied the effect of  $\text{Zn}^{2+}$  on the enzyme activity *in vitro*. The results showed that the inhibition of enzyme activity needed higher  $\text{Zn}^{2+}$  levels *in vitro* experiment. The value of  $\text{IC}_{50}$ ,  $\text{Zn}^{2+}$  concentration leading to 50% activity lost, was estimated to be  $6.00 \pm 0.25$  mM. Thus we thought that the toxicity of  $\text{Zn}^{2+}$  on the enzyme was due to the absorption and accumulation of  $\text{Zn}^{2+}$  to a certain level during the *in vivo* experiment. However, no accumulation process is involved during *in vitro* experiment, which suggests that the toxicity of  $\text{Zn}^{2+}$  on the enzyme is due to difference in  $\text{Zn}^{2+}$  concentrations between the *in vivo* and *in vitro* experiments.

In our investigations, the values of  $k_{\text{cat}}$  decrease with increasing  $\text{Zn}^{2+}$  concentrations. A slow and reversible inhibition reaction was observed at lower  $\text{Zn}^{2+}$  concentrations. The equilibrium constant was determined to be 11.92 mM using a standard Lineweaver–Burk plot. Applying the theory of the substrate reaction previously described by Tsou (18) and Xie et al. (19), the inhibition kinetics of prawn NAGase by  $\text{Zn}^{2+}$  at low con-

centrations was studied. The inhibitory equilibrium constant was determined to be 11.96 mM, which was accordant with that obtained from a standard Lineweaver–Burk plot. The kinetic results indicated that at pH 5.8, the action of  $\text{Zn}^{2+}$  on the enzyme was initially a quick equilibrium binding and then a slow inactivation. The microscopic rate constants were determined for inactivation and reactivation. The results showed that  $k_{+0}$  was much larger than  $k_{-0}$ , indicating the enzyme was completely inactivated at sufficiently large  $\text{Zn}^{2+}$  concentration. The inactivation rate constant of free enzyme approximately equaled to that of enzyme–substrate complex, which suggests that the substrate gave very little protection. The fluorescence emission spectra, CD spectra, and UV absorbance spectra are usually used to discuss the conformational changes of proteins after denaturation by denaturants, organic solvents, or heat (22, 23). In this article, we used the fluorescence emission spectra and UV absorbance spectra to assay the conformational changes of enzyme inactivated by  $\text{Zn}^{2+}$ . The results showed that the fluorescence emission peak and UV absorbance peak did not position shifted but the intensity decreased, indicating that the conformation of  $\text{Zn}^{2+}$ -bound inactive NAGase was stable and different from that of native NAGase. Zhang et al. (24) reported that ALPase from green crab (*Scylla serrata*) first quickly and reversibly bound  $\text{Zn}^{2+}$ , and then, in addition, underwent a slow course to inactivation. Increasing the  $\text{Zn}^{2+}$  concentration also had no significant red-shift of emission peak, but it caused the fluorescence emission intensity to increase (24). Han et al. (25) found that  $\text{Zn}^{2+}$  directly inhibited tyrosinase in a mixed-type manner accompanying conformational changes, which were reflected by the results of red-shift and decreases of the fluorescence intensity (25).

How  $\text{Zn}^{2+}$  induces the change of enzymatic activity and enzyme conformation? Maret et al. (26) presented that metallothionein could participate in the controlled delivery of zinc by binding it with high stability and by mobilizing it through a novel biochemical mechanism that critically depends on the redox activity of the zinc–sulfur bond. In green crab ALP, the enzyme active site also contains two  $\text{Zn}^{2+}$  ions and one  $\text{Mg}^{2+}$  ion, which can be removed by EDTA and are essential to the enzyme's function. Zhang et al. (24) thought that the  $\text{Zn}^{2+}$  ion was bound at the  $\text{Mg}^{2+}$  binding site which resulted in the inactivation of ALP and conformation change. Han et al. (25) considered that the ligand binding sites for  $\text{Zn}^{2+}$  would be furnished by the histidine or cysteine residues in tyrosinase. Kleina et al. (21) examined that both CI and CII domains of adenylyl cyclase bound  $\text{Zn}^{2+}$  with relatively high (submicromolar) affinity and induced the changes of enzyme activity and conformation. The *p*-hydroxymercuribenzoate and *p*-chloromercuribenzoate are special modifiers of SH group. Lynn (10) discovered that *p*-hydroxymercuribenzoate could strongly inhibit NAGase of the American lobster (*H. americanus*). Koga et al. (2) reported that  $\text{Hg}^{2+}$  could inhibit the silkworm (*B. mori*) NAGase activity. In our previous investigations, we found that  $\text{Hg}^{2+}$  could influence the conformation and activity of *L. vannamei* NAGase and only one molecule of  $\text{HgCl}_2$  binding with the

enzyme molecule could make irreversible inactivation of prawn NAGase (13). The histidine or cysteine residues are essential residues to prawn NAGase activity (13, 16). Therefore, we presumed that  $Zn^{2+}$  induced the changes of prawn NAGase activity and conformation by binding with the histidine or cysteine residues.

## ACKNOWLEDGEMENTS

This investigation was supported by the grant 30500102 of the Natural Science Foundation of China, the grant 2006N0067 of the Science and Technology Foundation of Fujian Province, and the grant 20070410806 of the China Postdoctoral Science Foundation.

## REFERENCES

1. Espie, P. J. and Roff, J. C. (1995) Characterization of chitinase from *Daphnia magna* and its relation to chitin flux. *Physiol. Zool.* **68**, 727–748.
2. Koga, D., Nakashima, M., Matsukura, T., Kimura, S., and Ide, A. (1986) Purification and properties of  $\beta$ -N-acetyl-D-glucosaminidase from alimentary canal of the silkworm, *Bombyx mori*. *Biol. Chem.* **50**, 2357–2368.
3. Koga, D., Shimazaki, C., Yamamoto, K., Inoue, K., Kimura, S., and Ide, A. (1987)  $\beta$ -N-Acetyl-D-glucosaminidase from integument of the silkworm, *Bombyx mori*: comparative biochemistry with the pupal alimentary canal enzyme. *Agric. Biol. Chem.* **51**, 1679–1681.
4. Scigelova, M. and Crout, D. H. G. (1999) Microbial  $\beta$ -N-acetylhexosaminidases and their biotechnological applications. *Enzyme Microb. Technol.* **25**, 3–14.
5. Funke, B. and Spindler, K. D. (1987) Developmental changes of chitinolytic enzymes and ecdysteroid levels during the early development of the brine shrimp *Artemia*. In *Artemia Research and its Applications* (Declair, C., ed.), pp. 67–78, Universa Press, Wetteren.
6. Cannon, R. D., Nimi, K., Jenkinson, H. F., and Shepherd, M. G. (1994) Molecular cloning and expression of the *Candida albicans*  $\beta$ -N-acetyl-D-glucosaminidase (HEX1) gene. *J. Bacteriol.* **176**, 2640–2647.
7. Zen, K. C., Choi, H. K., Krishnamachary, N., Muthukrishnan, S., and Kramer, K. J. (1996) Cloning, expression, and hormonal regulation of an insect  $\beta$ -N-acetyl-D-glucosaminidase gene. *Insect Biochem. Mol. Biol.* **26**, 435–444.
8. Peters, G., Saborowski, R., Mentlein, R., and Buchholz, F. (1998) Isoforms of an N-acetyl- $\beta$ -D-glucosaminidase from the Antarctic krill, *Euphausia superba*: purification and antibody production. *Comp. Biochem. Physiol. B Biochem. Mol. Biol.* **120**, 743–751.
9. Peters, G., Saborowski, R., Buchholz, F., and Mentlein, R. (1999) Two distinct forms of the chitin-degrading enzyme N-acetyl- $\beta$ -D-glucosaminidase in the Antarctic krill: specialists in digestion and moult. *Mar. Biol.* **134**, 697–703.
10. Lynn, K. R. (1990) Chitinases and chitinases from the American lobster (*Homarus Americanus*). *Comp. Biochem. Physiol. B Biochem. Mol. Biol.* **96**, 761–766.
11. Zou, E. and Fingerman, M. (1999) Chitinase activity in the epidermis and hepatopancreas of the fiddler crab *Uca pugilator* during the molting cycle. *Mar. Biol.* **133**, 97–101.
12. Esaiassen, M., Myrnes, B., and Olsen, R. L. (1996) Isolation and substrate specificities of five chitinases from the hepatopancreas of Northern shrimp, *Pandalus borealis*. *Comp. Biochem. Physiol. B Biochem. Mol. Biol.* **113**, 717–723.
13. Lin, J. C., Xie, X. L., Gong, M., Wang, Q., and Chen, Q. X. (2005) Effects of mercuric ion on the conformation and activity of *Penaeus vannamei*  $\beta$ -N-acetyl-D-glucosaminidase. *Int. J. Biol. Macromol.* **36**, 327–330.
14. Xie, X. L., Chen, Q. X., Lin, J. C., and Wang, Y. (2004) Purification and some properties of  $\beta$ -N-acetyl-D-glucosaminidase from prawn (*Penaeus vannamei*). *Mar. Biol.* **146**, 143–148.
15. Xie, X. L. and Chen, Q. X. (2004) Inactivation kinetics of  $\beta$ -N-acetyl-D-glucosaminidase from prawn (*Penaeus vannamei*) in the dioxane solution. *Biochemistry (Moscow)* **69**, 1675–1682.
16. Xie, X. L., Du, J., Huang, Q. S., Shi, Y., and Chen, Q. X. (2007) Inhibitory kinetics of bromacetic acid on  $\beta$ -N-acetyl-D-glucosaminidase from prawn (*Penaeus vannamei*). *Int. J. Biol. Macromol.* **41**, 308–313.
17. Yeh, S. T. and Chen, J. C. (2008) Immunomodulation by carrageenans in the white shrimp *Litopenaeus vannamei* and its resistance against *Vibrio alginolyticus*. *Aquaculture* **276**, 22–28.
18. Tsou, C. L. (1988) Kinetics of substrate reaction during irreversible modification of enzyme activity. *Adv. Enzymol. Relat. Areas Mol. Biol.* **61**, 381–436.
19. Xie, X. L., Gong, M., and Chen, Q. X. (2006) Inhibition kinetics of  $\beta$ -N-acetyl-D-glucosaminidase from prawn (*Penaeus vannamei*) by hydrogen peroxide. *J. Enzyme Inhib. Med. Chem.* **21**, 55–60.
20. Lowry, O. H., Rosebrough, N. J., Farr, A. L., and Randall, R. J. (1951) Protein measurement with the Folin phenol reagent. *J. Biol. Chem.* **193**, 265–269.
21. Kleina, C., Heyduka, T., and Sunahara, R. K. (2004) Zinc inhibition of adenylyl cyclase correlates with conformational changes in the enzyme. *Cell. Signal.* **16**, 1177–1185.
22. Chen, Q. X., Zhang, Z. Huang, H., Zhao, F. K., and Xu, G. J. (2003) Unfolding and inactivation of *Ampullarium crossean*  $\beta$ -glucosidase during denaturation by guanidine hydrochloride. *Int. J. Biochem. Cell Biol.* **35**, 1227–1233.
23. Wang, X. Y., Meng, F. G., and Zhou, H. M. (2004) Unfolding and inactivation during thermal denaturation of an enzyme that exhibits phytase and acid phosphatase activities. *Int. J. Biochem. Cell Biol.* **36**, 447–459.
24. Zhang, R. Q., Chen, Q. X., Xiao, R., Xie, L. P., Zeng, X. G., and Zhou, H. M. (2001) Inhibition kinetics of green crab (*Scylla serrata*) alkaline phosphatase by zinc ions: a new type of complexing inhibition. *Biochim. Biophys. Acta* **1545**, 6–12.
25. Han, H. Y., Zou, H. C., Jeon, J. Y., Wang, Y. J., Xu, W. A., Yang, J. M., and Park, Y. D. (2007) The inhibition kinetics and thermodynamic changes of tyrosinase via the zinc ion. *Biochim. Biophys. Acta* **1774**, 822–827.
26. Maret, W., Yetman, C. A., and Jiang, L. J. (2001) Enzyme regulation by reversible zinc inhibition: glycerol phosphate dehydrogenase as an example. *Chem. Biol. Interact.* **130**, 891–901.